ISBN: 978-3-95450-234-9 ISSN: 2673-5504 doi:10.18429/JACoW-SRF2023-WEIAA03

SURFACE ROUGHNESS REDUCTION AND PERFORMANCE OF Nb_3Sn FILM FOR SRF APPLICATIONS*

U. Pudasaini†, C. E. Reece, M. J. Kelley, E. M. Lechner, A.-M. Valente-Feliciano, O. Trofimova
Thomas Jefferson National Accelerator Facility, Newport News, VA, USA

Abstract

Nb_3Sn offers better RF performance (Q and E_{acc}) than Nb at any given temperature because of its superior superconducting properties. The potential deployment of Nb_3Sn-coated SRF cavities at 4 K, delivering similar performance to that of Nb cavities at 2 K, will be a transformational technology to enable new classes of SRF accelerator applications. A clean and smooth surface can enhance the performance of the Nb_3Sn-coated cavity, typically, the attainable acceleration gradient. The reduction of surface roughness is often linked with a correlative reduction in average coating thickness and grain size. A new approach to enhance the nucleation centers using the pre-deposition of Sn on Nb is introduced for surface roughness reduction. Besides Sn supply's careful tuning, the temperature profiles were varied to engineer the coating surface with reduced roughness as low as ~40 nm in 20 µm × 20 µm AFM scans, one-third that of the typical coating. Electropolishing of coated sample shows surface a clear surface smoothening. A few sets of coating parameters were used to coat 1.3 GHz single-cell cavities to understand the effects of roughness variation on the RF performance. This presentation discusses ways to reduce surface roughness with results from a systematic analysis of the samples and Nb_3Sn-coated single-cell cavities.

INTRODUCTION

Superior superconducting properties, Nb_3Sn (T_c ~ 18.33 K, H_{sh} ~ 425 mT, and Δ ~3.1 meV) promise better performance and a significant reduction in operational cost of SRF cavities compared to Nb (T_c ~ 9.2 K, H_{sh} ~ 210 mT, and Δ ~1.45 meV) [1]. So, it promises a higher accelerating gradient, quality factor, and operation temperature than traditional bulk Nb. Nb_3Sn superconducting radio frequency (SRF) cavities at 4.3 K can deliver similar performance to Nb cavities at 2 K, resulting in enormous cost savings for future SRF accelerators by simplifying and reducing the cost of cryogenic facilities. The successful deployment of Nb_3Sn technology can start a new era by benefiting numerous SRF accelerators and enabling new classes of SRF accelerator applications.

Despite Nb_3Sn being considered the next-generation SRF material, Nb_3Sn is restricted to its use in a thin film form because it is prone to develop cracks under stress because of its brittleness and the lower thermal conductivity that reduce the efficiency of dissipated heat removal from the cavity. Nb_3Sn thin films should be deposited or grown inside built-in metallic (e.g., Nb, Cu) cavity structures. Since SRF cavities typically have complicated geometries and demand uniformly coated surfaces, available thin film deposition techniques are limited to achieve them.

The Sn vapor diffusion coating is the most mature and, thus far, the only successful technique for growing quality Nb_3Sn on Nb cavities since the 1970s [2- 4]. In general, the essence of the process is to create and transport Sn-vapor to the Sn surface at suitable temperature environments. This technique is adopted by most research institutions currently working to develop Nb_3Sn-coated cavities around the world [5-9]. Recent performance results of such cavities are promising, attaining high quality factors, with > 10^{10} operating at 4.2 K at medium fields at ≥ 15 MV/m in several labs [5, 7, 10, 11]. The best-performing cavities have attained an accelerating gradient in excess of 20 MV/m. A typical cavity coating process consists of two steps: nucleation and growth. First, tin chloride is evaporated at about 500 ºC, depositing a Sn film and particles on the niobium surface to mitigate potential non-uniformity in the coating by depositing Sn improving nucleation [12]. These tin deposits act as nucleation sites, which are assumed to facilitate Nb_3Sn growth with the influx of tin vapor during deposition at a higher temperature. The growth temperature should be above 930 °C to exclusively form the Nb_3Sn phase as dictated by the binary phase diagram of the Nb-Sn system. A temperature of about 1100-1200 ºC is typical for Nb_3Sn growth at different labs.

The current understanding of performance limitations of Nb_3Sn-coated cavities is because of "extrinsic" factors such as localized defects. A few known issues that potentially contribute to performance limitations are forming very thin patchy regions, non-uniformity, accumulating Sn-residues, incorporating impurities, non-stoichiometric grain boundaries, surface topography, etc. It is needed to have pure Nb_3Sn with a clean and defect-free-smooth surface to enhance the performance. This contribution focuses on the roughness (or topography) of vapor-diffused Nb_3Sn and discusses ways to manage it with material analysis and RF test results.

VAPOR DIFFUSION COATING AND ROUGHNESS EVOLUTION

The quality of coated Nb_3Sn layers is mainly contingent on understanding the coating layer initiation and growth during the process. To understand the evolution of the Nb_3Sn thin film during the process, we ran a set of experi-

* Work supported by the U.S. Department of Energy, Office of Science, Office of Nuclear Physics under contract DE-AC05-06OR23177 with Jefferson Science Associates.
† uttar@jlab.org

ISBN: 978-3-95450-234-9 ISSN: 2673-5504 doi:10.18429/JACoW-SRF2023-WEIAA03

ments a few years ago, as described in [13]. A set of mechanically polished (nanopolished) Nb samples with an average roughness of < 5 nm from atomic force microscopy (AFM) scan size of 5 × 5 µm scans were coated. The outcomes at different stages of the coating were studied. After initiating the heating process with Sn and $SnCl_2$ inside a sample chamber, a sample was coated for 1 h at 500 °C, finishing the nucleation stage. The other three samples were further heated to the coating temperature of 1200 °C for 5 min, 1 h, and 3 h; more details are available in [14]. The representative AFM images obtained from each sample are shown in Fig. 1. The roughness estimation from 4-5 AFM scans resulted in average roughness of 54.8 ± 9.4 nm for the sample after the nucleation stage. The average roughness was 7.3 ± 0.6, 23.6 ± 4.6, and 61.8 ± 4.6 nm for the sample coated for 5 min, 1 h, and 3 h, respectively. The surface roughness is higher due to the distribution of Sn-islands of height up to ~90 nm after the nucleation. As the coating progresses, Sn particles on the surface convert into Nb_3Sn grains, resulting in a uniform coating layer. The evolution of grain size and topography with the coating time is clear. The grain size of a few tens of nm after 5 min of coating time changes into a few hundred nm after 1 h and about a micron after 3 h. As the coating grows, the roughness grows with it, along with the reduction in the number of grains. The interrelation between the grain size, thickness, and roughness will be discussed in a later section.

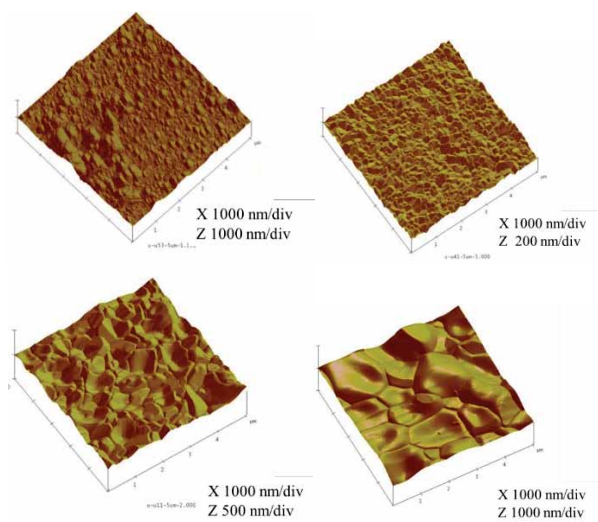

Figure 1: The evolution of surface topography with the coating growth. AFM images were obtained from sampled coated for 1 h at 500 ºC and an additional 5 min, 1 h, and 3 h at 1200 ºC, respectively.

The roughness of the vapor diffused Nb_3Sn is typically contributed by the grain boundaries' channeling, depression in the middle of the grain, grain faceting, and other contributing factors, including pits and void formation and condensation of Sn-residues. The distribution of features like sharp edges, pits, and protrusions on the surface will likely enhance the surface magnetic fields above the critical field [15, 16]. This can lead to quenching the whole cavity.

An AFM image taken from a witness sample coated with a cavity along with a sectional height profile is shown in Fig. 2, where grain boundaries, voids, grain size distribution, depression, and protrusion in the grain can be seen.

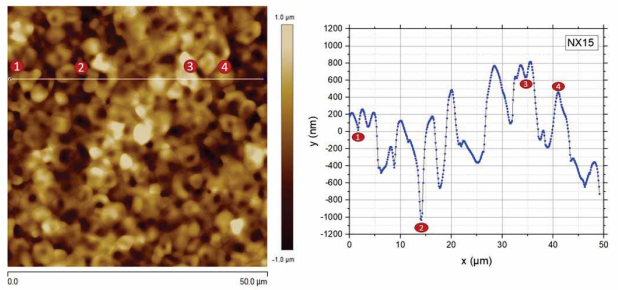

Figure 2: AFM image from a Nb_3Sn-coated cavity witness sample (left) and corresponding sectional height profile (right). Labels 1, 2, 3, and 4 show the position of grain boundary, void, depression, and grain protrusion, respectively, and the corresponding variation in the surface roughness. It has been observed that the grain boundary channel (e.g., 2) gets deeper with grain size increase.

ROUGHNESS AND PERFORMANCE OF Nb_3Sn CAVITIES

Fermilab reported the performance of a record Nb_3Sn-coated cavity achieving 22.5 MV/m with Q ~10^{10} up to ~20 MV/m in SRF 2019 [11, 17], which was credited to relatively thin shiny coating with a very low surface roughness that was produced with a new coating process that included a modified high-temperature nucleation step.

In the "Siemen configuration" with no secondary heater, adopting and studying such coating protocols was not feasible at JLab. From our sample studies, we have observed the variation in grain sizes, roughness, and thickness but had not yet tested in actual cavity coating. In 2021, leveraging the previous studies, we reduced the coating duration at 1200 °C and implemented a "three-step" temperature profile to avoid Sn-residues. Although the residue removal was not entirely successful, the coating observed in the cavity was smoother than usual [18].

The cavity, TE1NS002 performed well with low field Q_0 about 2.5×10^{10} at 4.3 K and 1×10^{11} at 2 K, followed by a mild Q-slope present with a quench field >17 MV/m at 4 K $Q_0 > 10^{10}$. Further analysis of the witness samples revealed that even the better-performing cavities in the past, such as RDT7, reported in SRF 2019 [7], had lower surface roughness. Table 1 below summarizes test results from several cavity coating experiments coated in the course of different studies. The average surface roughness of the witness sample is typically correlated with the achievable maximum accelerating gradient. Cavities with no significant Q-slope (e.g., RDT7, TE1NS002) have the lowest surface roughness. Even with observed Sn-residues, others have achieved maximum accelerating gradients close to 20 MV/m with Q-slope. Note that the improvement in the attainable gradient could be the combination of the smoother surface and the thinner coating; the first can result in less heating in the surface, and, due to the lower

ISBN: 978-3-95450-234-9 ISSN: 2673-5504 doi:10.18429/JACoW-SRF2023-WEIAA03

thermal conductivity of Nb_3Sn, a thinner layer is more efficient removing in terms of dissipated heat than a thicker one.

Table 1: Performance of single-cell cavity coated with Nb_3Sn with varying surface roughness. Average Roughness values are estimated from 20 µm× 20 µm AFM scans from 3-4 areas of each sample.

Cavity	Low field Q at 4.3 K	E_{acc} with $Q > 10^{10}$ at 4.3 K	Max E_{acc} (MV/m)	Ra (nm)
RDT7	3×10^{10}	15.5	15.5	57 ± 4
TEN1S002	2.5×10^{10}	16.5	17.5	68 ± 3
P4P5	1.3×10^{10}	10	20.7*	98 ± 4
TE1NS001	1.6×10^{10}	11	18.9	87 ± 4
TE1NS001	2.3×10^{10}	9.5	16	102 ± 16
TE1NS001	1.7×10^{10}	9	16.5	154 ± 10
TE1NbSn01	1.3×10^{10}	7.5	19.2*	77 ± 1

CORRELATION BETWEEN ROUGHNESS, GRAIN SIZE, AND THICKNESS

The roughness increases along with the growth of the coating during the process, as discussed above. Figure 3 shows thin film thickness, surface roughness, and grain size measured from samples coated in identical coating setups by varying the coating time and temperatures. A positive correlation between the growth of the thin film with increasing grain size and the surface roughness can be observed. Similar data were reported before from our group and others [11, 19]. The trend was typically followed for many coatings prepared with different coating conditions with known coating layer thickness.

ROUGHNESS REDUCTION

Grain size or thickness variation directly affects the roughness of as-coated Nb_3Sn. Since roughness correlates with grain size and film thickness, we seek to design a coating process that minimizes roughness by tuning the nucleation and coating growth parameters. Our previous study showed that varying the nucleation parameters using $SnCl_2$ has no significant effect on the microstructure of the final coating [12]. The pre-deposition of a thin Sn-layer on the substrate before the coating was examined, aiming at a high nucleation center density for uniform coating growth to reduce the surface roughness. Following our previous sample studies, the microstructures can be controlled by adjusting the coating parameters that can be leveraged to obtain a coating with desired microstructures for smoother coating. Here we discuss an alternate way to enhance the nucleation by depositing a thin Sn-layer on Nb before the deposition and adjusting the coating parameters. Another way is to manage the roughness with post-processing techniques. We present some results from a recent electropolishing experiment.

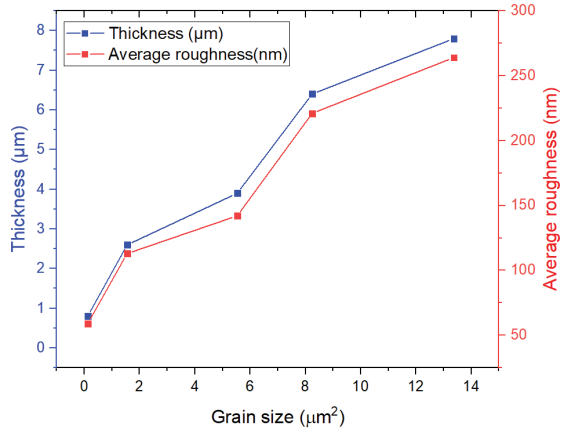

Figure 3: The variation roughness and thickness with grain size of vapor diffused Nb_3Sn. Average surface roughness values were measured from 50 µm × 50 µm AFM scans.

Pre-Deposition of the Sn Layer

The current understanding of the Nb_3Sn thin-film growth is that Sn particles and ultra-thin Sn-films are deposited on the surface during the nucleation stage via $SnCl_2$ dissociation, which initiates the formation of Nb_3Sn nucleation sites required for the uniform coating. These nucleation sites initiate the growth of Nb_3Sn grains and grow until all the grains are connected and cover the Nb surface with a layer of Nb_3Sn. Then the Nb_3Sn growth proceeds at the Nb_3Sn-Nb interface, so subsequent growth occurs via grain boundary diffusion of Sn.

The distribution of nucleation sites impacts the grain size distributions and the roughness. Without sufficient nucleation sites, it will likely develop 'patchy' regions (large thin grains). One can imagine that a compact uniform distribution of nucleation sites can lead to homogeneous grain sizes with lower roughness with generous grain boundary density for the growth of the coating.

A set of Nb samples was subjected to a typical vapor diffusion coating protocol. Sn layers of 0 nm, 10 nm, 20 nm, and 1 µm were deposited before the coating using the magnetron sputtering technique in a separate coating system [20]. The details on the Nb_3Sn coating protocol are available in [18]. The sample with pre-deposited 1 µm thick Sn was placed outside the sample chamber, packaged tightly inside a Nb foil refraining from Sn vapor, allowing the coating to grow from the Sn on the surface. The atomic force microscopy (AFM) images obtained from the sample with and without pre-deposited Sn-layer, shown in Fig. 4, show the topography variation between samples. Table 2 summarizes average grain size and roughness estimations, showing a significant roughness reduction sample with pre-deposited Sn than the regular sample with no prior Sn deposition.

The roughness and grain size were reduced more with a thicker Sn layer on the pre-coated sample. Note the reduction in the standard deviation associated with measured roughness measurements, with increased thickness of Sn-layer showing more homogeneous coating in the sample

ISBN: 978-3-95450-234-9 ISSN: 2673-5504 doi:10.18429/JACoW-SRF2023-WEIAA03

with 20 nm deposited layer of Sn. The reduction in roughness or the grain size in the pre-deposited Sn layers is likely due to improved nucleation with available Sn from the beginning, resulting in more grains in the beginning.

The Nb sample with pre-deposited 1 µm Sn thickness was also analyzed. Since the sample wrapped inside an Nb foil was not sitting flat, the same area appeared to have melted Sn. Several areas on the sample surface showed dense small grains; the roughness values were typically ~50 nm in these areas. Another Nb sample in the same foil exposure indicated Sn evaporation from the surface during the thermal treatment. Thermal conversion of electrodeposited Sn on Nb into Nb_3Sn inside a single-cell Nb cavity is already underway, resulting in significantly smoother coatings than vapor-diffused coating [21].

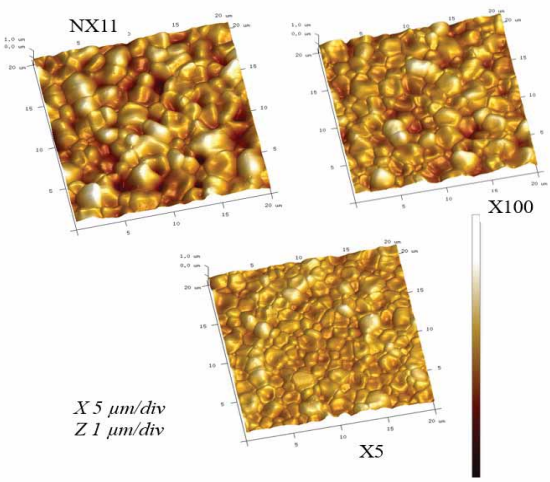

Figure 4: AFM images from Nb_3Sn grown on Nb sample (NX11) and Nb with pre-deposited Sn layer of thickness 10 nm (X100) and 20 nm (X5). Note the variation of surface roughness with and without pre-deposited Sn layers.

Table 2: Average roughness and grain sizes of Nb_3Sn grown on regular Nb sample and Nb with pre-deposited Sn layers.

Samples	Thickness of pre-deposited Sn (nm)	Average grain size (µm)	Average roughness R_a (nm)
NX11	0	1.85 ± 0.14	180 ± 32.4
X100	10	1.52 ± 0.10	125 ± 22.6
X5	20	1.26 ± 0.07	83 ± 3.12

Tuning Coating Parameters

We previously reported results from investigating several factors that influence Sn supply and consumption during the Nb_3Sn film growth affecting the thin film's microstructures [18]. Depending on the source size and the substrate area, one can carefully tailor desired microstructure by modifying a temperature profile or the available Sn flux. We examined the roughness of the coating for a fixed coating temperature profile by varying the size of Sn-crucibles for a constant volume or changing the coating volume to fix the source sizes. Table 3 shows the grain size and roughness variation as a function of the size of the Sn crucible for samples coated with identical coating parameters. It can be seen that as the crucible size or the Sn-flux increases, it results in larger grain sizes and surface roughness. A similar trend was observed while the Sn source was fixed, and the substrate area was varied.

Table 3: Roughness and Grain Size Variation with Sn Consumption

Diameter (inch)	Cross-sectional area (cm^2)	Sn use (g)	Grain size (µm)	Average Roughness Ra (nm)
1.0	5.07	0.81	1.63± 0.02	126 ± 1.0
0.5	1.27	0.33	1.21± 0.06	95.8±3.4
0.25	0.32	0.10	0.56± 0.02	28.2± 3.3

The latest standard coating process for a single-cell cavity at JLab consists of 90-minute nucleation at ~540 °C followed by three temperature steps; 40 min, 45 min, and 85 min coating at 1200 °C, 1150 °C and 1100 °C, respectively. In a set of experiments, the temperature profiles were shortened by changing the time for different temperatures aiming at a thinner coating for a smoother surface. Samples were coated inside a mock cavity using the temperature profile shown in Table 4 by keeping the nucleation profile, amount of Sn (~ 1 g), and $SnCl_2$ (~ 0.5 g) constant.

Table 4: Temperature profiles used for the coating and measured average surface roughness, grain size, and thickness.

	1200 °C	1150 °C	1100 °C	Sample	Ra (nm)	Grain size (µm)	Thickness (µm)
01	10 min	45min	85min	CW36	69 ± 3	0.93	-
02	10 min	45min	-	CW44	40 ±1	0.75	1.0 ± 0.2
03	10 min	-	-	CW20	27 ±2	0.55	0.75 ± 0.15
04	10 min	-	85min	CW07	43.5±1.5	0.6	1.02+/0.17

Figure 5 shows the 20 µm × 20 µm AFM images from samples in Table 3. It can be seen that a longer coating cycle results in relatively larger grains and higher surface roughness, as expected. The growth of ~ 1 µm thick Nb_3Sn coating with an average surface roughness of 40-50 nm would be particularly appealing for SRF cavity coating. No non-uniformity or 'patchy' region formation was observed in these sample experiments.

Following the sample studies, a 1.3 GHz single-cell cavity, TE1Nb_3Sn02, was coated following a similar coating protocol used to coat sample CW36. The visual inspection after the cavity coating revealed some asymmetry between the two half-cells. The half-cell visible from the top, out-of-sight from the Sn sources, showed some shiny features which looked like the edges of underlying Nb grain boundaries but coated. The witness sample hung from the top has 'patchy regions' unlike another sample at the bottom, as shown in Fig. 6. The roughness measured from these samples was 80±10 nm, which was not as smooth as aimed for

ISBN: 978-3-95450-234-9 ISSN: 2673-5504 doi:10.18429/JACoW-SRF2023-WEIAA03

compared to CW36. We believe the short coating period at 1200 °C was insufficient for uniform nucleation at the beginning of the coating growth.

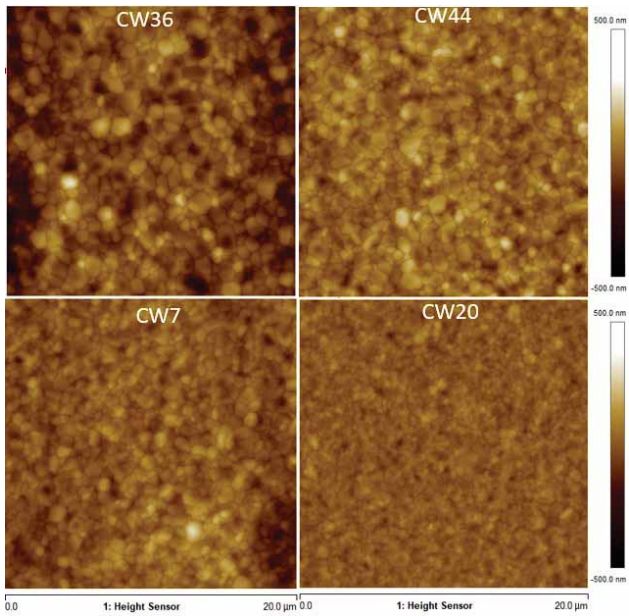

Figure 5: AFM images obtained from samples coated with temperature profiles listed in Table 4.

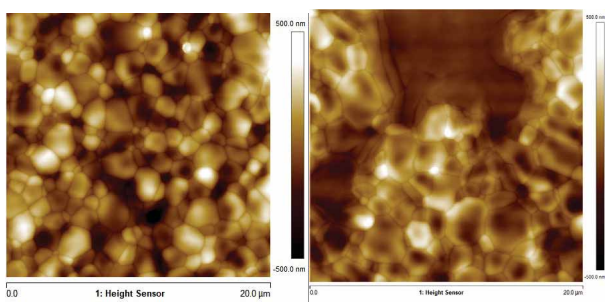

Figure 6: AFM images from the witness sample coated with TE1Nb3Sn02 placed inside at the bottom and top, respectively. Note the patchy region on the sample hung from the top on the right.

Despite the patchy regions, the cavity was tested at 4.3 K and 2 K; see Fig. 7. The Q-values were lower than expected at both temperatures, dominated by the residual resistance. A reproducible Q-switch was observed at ~ 12 MV/m, resulting in a partial quench degrading the Q-factor; eventually, the test was limited by the input RF power. The Q switch was absent in the 2 K test, indicating the partial quench in the 4.3 K test was a thermal phenomenon. The cavity was measured up to 18.8 MV/m, limited by available rf power and exhibited a Q-slope. It is possible that the thinner and smoother coating may have helped to attain such a gradient despite the presence of 'patchy' and visible shiny features. We have coated a couple of additional cavities and avoided the non-uniformity in a visual inspection and will be testing soon.

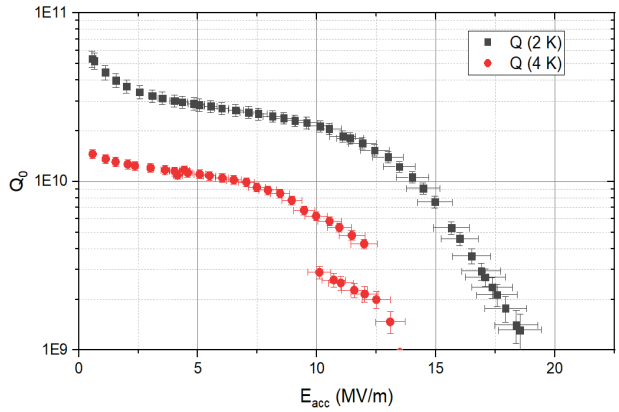

Figure 7: Performance of a 1.3 GHz single-cell cavity following the coating temperature profile, first in Table 4.

Electropolishing

The previous section discussed potential ways to grow smoother vapor-diffused Nb_3Sn film. Because of the complication of the bi-elemental composition, the limited thickness of the material, and brittleness, the post-coating polishing techniques are challenging. Despite a burst of initial efforts, the effort had subsided for several years. Fermilab researchers are working to develop mechanical polishing using centrifugal barrel polishing, where the initial results are exciting [22]. We recently revisited the electropolishing process with a Nb_3Sn-coated Nb sample by sequentially removing thin layers of Nb_3Sn [23]. A set of mechanically polished samples was coated after the final substrate surface preparation. These samples were subjected to 150 nm EP removal. For the treatment, a voltage of 9 V was used, resulting in ~ 20 mA/cm^2 current density. The chosen voltage was higher than the previous EP experiments at 6.5 V. AFM images captured from as-coated and EP-treated same samples are shown in Fig. 8. The polishing of the sample is evident with a reduction in roughness from 161 nm to 121 nm in 20 µm × 20 µm scans and 93 nm from 142 nm. Some "scratch-like" features appeared on the surface following the EP, along with some particles. EDS analysis revealed nothing besides Nb, Sn, and their oxides. The sequential EP removal showed that the coating degraded from these "scratch-like" features and was exposed to substrate faster than other areas. Since these defects appear randomly, their origin needs to be understood, which we plan to investigate further.

SURFACE ROUGHNESS AND ACCELERATING GRADIENT

As shown in Fig. 2, the topographical features of as-coated Nb_3Sn could be a major factor contributing to the current limitations in the Nb_3Sn-coated cavity. During the growth of the film, it seems to develop voids, depressions, protrusions, facets, and deep grain boundary channels with

ISBN: 978-3-95450-234-9 ISSN: 2673-5504 doi:10.18429/JACoW-SRF2023-WEIAA03

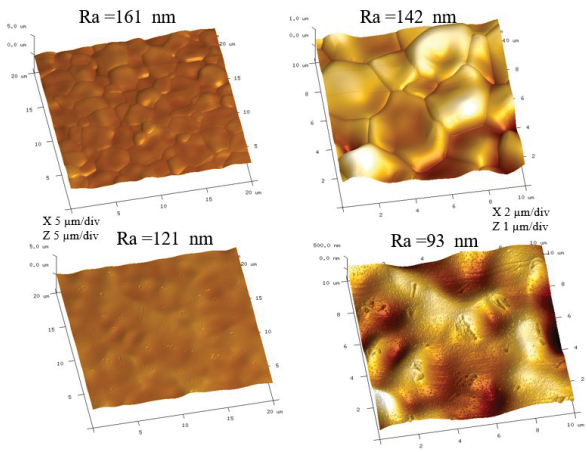

Figure 8: Surface roughness reduction following 150 nm EP Nb_3Sn-coated samples. AFM images from as-coated and same sample EP'ed are in the top and bottom rows, respectively.

thermally grooved grains [13]. This presents a vulnerability to enhancing the magnetic field [24] at or suppressing the superheating field at the grain boundary [16, 25]. Roughness or grain size may be used as a metric to estimate accelerating gradient since surface roughness scales with grain size, as shown in Fig. 9(a). The increase in surface roughness may also explain the increasing width of the distribution of magnetic field enhancement factors, β, as shown in Fig. 9(b).

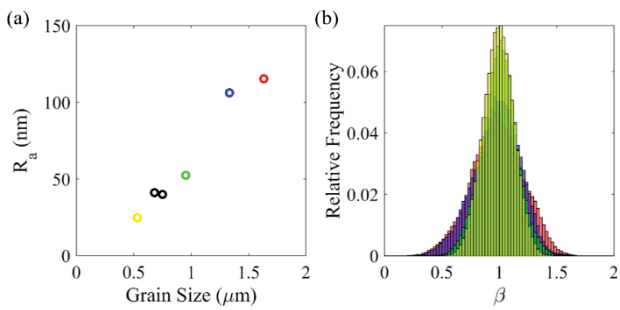

Figure 9: (a) Measurement of surface roughness, R_a, as a function of grain size. (b) Relative frequency of the magnetic field enhancement factor calculated from AFM topographies using a perfect electrical conductor model. The colors shared between (a) and (b) indicate measurements derived from the same AFM topography.

We have coated several single-cell cavities and monitored roughness, as summarized in Table 1. A qualitative correlation between the roughness and attainable accelerating gradient seemed to exist, as suggested in Fig. 9. Despite the problem of Sn residues or even patchy regions, single-cell cavities reach ~ 19 MV/m more frequently. The performance of two representative single-cell cavity test results is shown in Fig. 10. Both cavities were coated several times before, but the gradient was maximum when the surface roughness estimated from the witness sample was minimum. The larger error bars in the low-field test data for P4P5 are due to a highly over-coupled input antenna. This cavity reached the maximum gradient of 20.6 MV/m at 2 K with no quench; the input power limited both tests at 2 K and 4 K.

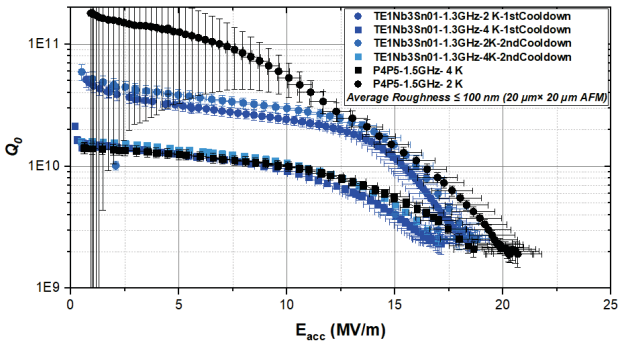

Figure 10: Performance of two single-cells with estimated average roughness <100 nm in the corresponding witness samples.

SUMMARY AND OUTLOOK

There is a well-accepted notion that SRF cavity surfaces must be "pure," "clean," and "smooth" for optimal performance. If ~1 μm coating is deposited by adjusting these parameters, it could improve the performance by reducing the losses because of the roughness and making heat removal more efficient than the thicker coating of poor conducting Nb_3Sn. Since the surface roughness of Nb_3Sn films grows as the thin film grows thicker along with the grain size, one way to manage the topography is to vary the coating parameters such as coating time, temperature and time, Sn-flux, etc. The surface roughness reduction by varying the coating parameters can be made carefully, avoiding a marginally thin coating. We showed that depositing a thin layer of Sn before the coating makes it possible to produce even smoother surfaces by creating homogeneous nucleation without compromising the coating thickness. A plan is in place to implement this to a 2.45 GHz single-cell cavity using this hybrid technique. Sn will be sputtered into a cavity and subjected to typical vapor diffusion. We presented some results from the electropolished Nb_3Sn-coated sample. Despite the promising roughness reduction, more studies are needed to understand the surface defects, their effect on performance, and surface chemistry.

ACKNOWLEDGMENTS

We thank Dr. Nizam Sayeed for depositing Sn on Nb samples at Old Dominion University Applied Research Center, and Carrie Baxley for the help with sample EP. AFM measurement was done at Applied Research Center Core Labs, The College of Willam & Mary.

REFERENCES

[1] H. Padamsee, J. Knobloch, and T. Hays, *RF Superconductivity for Accelerators,* Wiley & Sons, New York, 1998.

[2] G. Arnolds and D. Proch, "Measurement on a Nb_3Sn structure for linear accelerator application", *IEEE Trans. Magn.*, vol. 13, pp.500-503, 1977. doi:10.1109/TMAG.1977.1059387

ISBN: 978-3-95450-234-9 ISSN: 2673-5504 doi:10.18429/JACoW-SRF2023-WEIAA03

[3] P. Kneisel *et al.,* "Measurements of superconducting Nb_3Sn cavities in the GHz range", *IEEE Trans. Magn.*, vol. 15, no. 1, pp. 21-24, 1979. doi:10.1109/TMAG.1979.1060193

[4] G. Mueller, P. Kneisel, D. Mansen, H. Piel, J. Pouryamout, and R. Roeth, "Nb3Sn Layers on High-Purity Nb Cavities with Very High Quality Factors and Accelerating Gradients", in *Proc. EPAC'96*, Sitges, Spain, Jun. 1996, paper WEP002L, pp. 2085-2087. https://jacow.org/e96/PAPERS/WEPL/WEP002L.PDF

[5] R. D. Porter *et al*., "Next Generation Nb_3Sn SRF Cavities for Linear Accelerators", in *Proc. 29th Linear Accelerator Conf. (LINAC'18)*, Beijing, China, Sep. 2018, pp. 462-465. doi:10.18429/JACoW-LINAC2018-TUPO055

[6] S. Posen *et al., "*Development of Nb_3Sn Coatings for Superconducting RF Cavities at Fermilab. No. FERMILAB-CONF-18-477-TD". Fermi National Accelerator Lab. (FNAL), Batavia, IL, USA, 2018.

[7] G. Eremeev *et al.,* "Nb_3Sn multi-cell cavity coating system at Jefferson Lab", *Rev. Sci. Instrum.*, vol. 91, p. 0739112020. doi:10.1063/1.5144490

[8] Z. Q. Yang *et al*., "Development of Nb_3Sn Cavity Coating at IMP", in *Proc. 19th Int. Conf. RF Superconductivity (SRF'19)*, Dresden, Germany, Jun.-Jul. 2019, pp. 21-24. doi:10.18429/JACoW-SRF2019-MOP003

[9] K. Takahashi *et al*., "First Nb_3Sn Coating and Cavity Performance Result at KEK", in *Proc. SRF'21*, East Lansing, MI, USA, Jun.-Jul. 2021, p. 27. doi:10.18429/JACoW-SRF2021-SUPCAV009

[10] U. Pudasaini, J. W. Angle, G. V. Eremeev, M. J. Kelley, C. E. Reece, and J. Tuggle, "Nb_3Sn Films for SRF Cavities: Genesis and RF Properties", in *Proc. 19th Int. Conf. RF Superconductivity (SRF'19)*, Dresden, Germany, Jun.-Jul. 2019, pp. 810-817. doi:10.18429/JACoW-SRF2019-THFUA6.

[11] S. Posen *et al.,* "Advances in Nb_3Sn superconducting radiofrequency cavities towards first practical accelerator applications", *Supercond. Sci. Technol.* vol. 34, p. 025007, 2021. doi:10.1088/1361-6668/abc7f7

[12] U. Pudasaini *et al.,* "Initial growth of tin on niobium for vapor diffusion coating of Nb_3Sn", *Supercond. Sci. Technol.,* vol. 32, p. 045008, 2019. doi:10.1088/1361-6668/aafa88

[13] U. Pudasaini *et al.,* "Growth of Nb_3Sn coating in tin vapor-diffusion process", *J. Vac. Sci. Technol.A: Vac., Surf., Films,* vol.37, p. 051509, 2019. doi:10.1116/1.5113597

[14] U. Pudasaini, M. J. Kelley, G. V. Eremeev, and C. E. Reece, "Local Composition and Topography of Nb3Sn Diffusion Coatings on Niobium", in *Proc. SRF'15*, Whistler, Canada, Sep. 2015, paper TUPB054, pp. 703-707. https://jacow.org/SRF2015/papers/TUPB054.pdf

[15] T. Kubo, "Magnetic field enhancement at a pit on the surface of a superconducting accelerating cavity", *Prog. Theor. Exp. Phys.,* vol. 2015, no.7, 2015. doi:10.1093/ptep/ptv088

[16] T. Kubo, "Field limit and nano-scale surface topography of superconducting radio-frequency cavity made of extreme type II superconductor", *Prog. Theor. Exp. Phys., v*ol. 2015, no. 6, 2015. doi:10.1093/ptep/ptv082

[17] S. Posen *et al.*, "Nb_3Sn at Fermilab: Exploring Performance", in *Proc. SRF'19*, Dresden, Germany, Jun.-Jul. 2019, pp. 818-822. doi:10.18429/JACoW-SRF2019-THFUB1

[18] U. Pudasaini, C. E. Reece, and J. K. Tiskumara, "Managing Sn-Supply to Tune Surface Characteristics of Vapor-Diffusion Coating of Nb_3Sn", in *Proc. SRF'21*, East Lansing, MI, USA, Jun.-Jul. 2021, p. 516. doi:10.18429/JACoW-SRF2021-TUPTEV013

[19] U. Pudasaini, M. J. Kelley, G. V. Eremeev, C. E. Reece, and J. Tuggle, "Effect of Deposition Temperature and Duration on Nb_3Sn Diffusion Coating", in *Proc. IPAC'18*, Vancouver, Canada, Apr.-May 2018, pp. 3950-3953. doi:10.18429/JACoW-IPAC2018-THPAL130

[20] MN Sayeed, H. Elsayed-Ali, G. V. Eremeev, M. J. Kelley, C. E. Reece, and U. Pudasaini, "Magnetron Sputtering of Nb_3Sn for SRF Cavities", in *Proc. IPAC'18*, Vancouver, Canada, Apr.-May 2018, pp. 3946-3949. doi:10.18429/JACoW-IPAC2018-THPAL129

[21] Z. Sun *et al.,* "Smooth, homogeneous, high-purity Nb_3Sn RF superconducting films by seed-free electrochemical synthesis", 2023. doi:10.48550/arXiv:2302.02054

[22] E. Viklund, D. N. Seidman, D. Burk, and S. Posen, "Improving Nb_3Sn Cavity Performance Using Centrifugal Barrel Polishing", 2023. doi:10.48550/arXiv:2305.10226

[23] U. Pudasaini, M. J. Kelley, G. V. Eremeev, C. E. Reece, and H. Tian, "Electrochemical Finishing Treatment of Nb_3Sn Diffusion-coated Niobium", in *Proc. SRF'17*, Lanzhou, China, Jul. 2017, pp. 900-905. doi:10.18429/JACoW-SRF2017-THPB070

[24] C. Xu *et al.,* "Simulation of nonlinear superconducting rf losses derived from characteristic topography of etched and electropolished niobium surfaces", *Phys. Rev. Accel. Beams,* vol. 19, 2016, p. 033501. doi:10.1103/PhysRevAccelBeams.19.033501

[25] E.M. Lechner, J.W. Angle, C. Baxley, M.J. Kelley and C.E. Reece, "Topographic Evolution of Nitrogen Doped Nb Subjected to Electropolishing", presented at SRF'23, Grand Rapids, MI, USA, Jun. 2023, paper MOPMB044, this conference.